Whole transcriptome analysis of the differential RNA profiles and associated competitive endogenous RNA networks in hyperuricemia-induced mild cognitive impairment (MCI)

Xiaoni Shao (xnshao@swun.edu.cn)
College of Pharmacology, Southwest Minzu University
Pengke He
College of Pharmacology, Southwest Minzu University
Na Li
College of Pharmacology, Southwest Minzu University
Mukaram Amatjana
College of Pharmacology, Southwest Minzu University
Boheng Zhang
College of Pharmacology, Southwest Minzu University
Xianyan Mai
College of Pharmacology, Southwest Minzu University
Qianle Jiang
College of Pharmacology, Southwest Minzu University
Haochen Xie
Qinghai Tibet Plateau Research Institute, Southwest Minzu University

Research Article

Keywords: Hyperuricemia, Mild cognitive impairment, Hippocampus, Whole transcriptome, Rats

Posted Date: April 5th, 2022

DOI: https://doi.org/10.21203/rs.3.rs-1463932/v1

Abstract

Background: Aimed at investigate the dysregulated genes, pathways and networks involved in hyperuricemia-induced mild cognitive impairment (MCI) through performing whole transcriptome sequencing, revealing the potential mechanism of hyperuricemia-induced MCI.

Results: A total of 463 DEGs, including 391 mRNA, 31 lncRNA, 8 cirRNA, and 33 miRNA were differentially expressed in HUA rats compared with the common rats by calculating the gene fragments per kilobase million (FPKM) in each sample and conducting differential gene analysis. The GO enrichment analysis showed 10 GO terms were significantly enriched, and the KEGG pathway enrichment analysis showed ECM-receptor interaction, PI3K-Akt signaling pathway, protein digestion and absorption, neuroactive ligand-receptor interaction and morphine addiction were significantly enriched.

Conclusions: Hyperuricemia can cause a certain degree of abnormal gene expression and modulate signaling pathways in the hippocampus.

Background

Hyperuricemia (HUA) is a symptom of high uric acid (UA) caused by excessive UA production or decreased excretion. HUA is a metabolic problem that has become increasingly common worldwide, and its association with hypertension has been studied for more than 130 years [1]. UA is the end product of purine metabolism, which is predominantly performed by the proximal tubules [2]. Two main sources of purine in humans have been identified: one is the synthesis of endogenous purine, and the other is the intake of a purine-rich diet [3, 4]. Purines are natural compounds present in all cells of the body and substantially all eatables [5]. If the intake of seafood and meat is too high, high levels of serum uric acid (SUA) may occur, but the total protein consumption is not [6]. SUA is the most plentiful spontaneous antioxidant in human plasma [7]. Its antioxidant properties prevent damage caused by free radicals, reducing the risk of MCI and dementia associated with oxidative stress [8]. Normally, 30% of UA in the human body is excreted from the intestine and bile duct, and 70% is excreted through the kidney [9, 10]. HUA was defined as a UA concentration > 7.0 mg/dl [11–13]. Although SUA seems to be a significant antioxidant in the human body and is thought to protect the human body when present at normal levels, an in-depth analysis of whether UA is adversely active, acting as a pro-oxidant and activator of phlogistic pathways, is needed [14–18]. The body maintains a balance between the production and excretion of UA every day to maintain the normal level of UA. In recent years, the incidence of HUA has increased rapidly [19, 20].

Despite increasing evidence for a direct correlation of HUA with cognitive function, our understanding of the syndrome is limited, and few therapeutic options are available [21]. In recent research, scholars found that HUA exerts a certain effect on cognitive function [22]. We chose to generate a rat model by feeding them special diets. Extensive evidence has shown the validity of the Morris water maze (MWM) as a method for assessing hippocampus-dependent reference memory and spatial guidance [23], its specificity as an evaluation of place memory, and its relative immunity to motivational differences across a series of experimental therapies that are secondary to the key purpose of the study, such as pharmacological treatment, lesions, and genetic manipulation. Therefore, after the model was successfully established, we administered an MWM test to all rats to assess the effects of HUA on MCI. We measured the blood biochemical parameters of all rats to confirm the successful establishment of the model. Then, we performed a whole transcriptome analysis of rat hippocampal tissues after the modeling cycle. The hippocampus is a component of the limbic system in the brain, and the exact location is

between the thalamus and medial temporal lobe. The hippocampus is mainly responsible for the storage, orientation and conversion of long-term memory [24].

A whole transcriptome analysis aims to assess the sum of all RNA that a particular cell can transcribe in a particular state and involves mRNA and noncoding RNA (ncRNA) [25]. Research on ncRNAs mainly focuses on miRNAs, lncRNAs and circRNAs, with regulatory effects identified based on second-generation sequencing technology. The whole transcriptome sequence is studied, and mRNAs, lncRNAs, circRNAs, and miRNAs are analyzed. Through a pairwise association analysis, ternary association analysis and multivariate association analysis, the research is more systematic, and the changes in transcriptional regulation underlying biological phenomenon are explored in depth.

Previous studies have claimed that UA in human vascular cells and endothelial cells upregulates C-reactive protein (CRP), an inflammation marker [26, 27]. Furthermore, various illnesses caused by HUA are related to activation of the Toll-like receptor 4 (TLR4)/nuclear factor (NF)-κB signaling pathway [22]. TLRs are important protein molecules involved in nonspecific immunity (innate immunity) and a bridge between nonspecific immunity and specific immunity [28]. Based on accumulating evidence, UA-induced activation of TLR4 damages hippocampus-dependent spatial relation memory in an inflammation-dependent manner and diminish the hippocampal pyramidal neuron dendrite length [29, 30]. An erstwhile study suggested that SUA functions as a mighty inflammatory stimulus that is transported across the blood-brain barrier [23, 31]. A few studies have shown that an increase in UA levels might affect cognitive functioning by inducing cerebrovascular changes [32, 33]. Here, we established a HUA model in which rats were provided with a high-UA diet (HUAD) and were used as the experimental group, while the rats in the control group were provided with normal basic feed as the control group. RNA-seq was used to identify differentially expressed RNAs and methodically analyze the genetic background of HUA-induced MCI. We found that HUA altered gene expression in the hippocampus and modulated a series of signaling pathways to induce encephalopathy.

We construct models to explore the real cause of the effects of HUA on the function of the hippocampus and to identify the specific targets. In summary, in this study, we performed whole-transcriptome sequencing to screen the differentially expressed mRNAs, lncRNAs, miRNAs and circRNAs. Therefore, based on the bioinformatics analysis, mRNA-lncRNA-miRNA networks were established, and then we identified the biological functions of the target genes.

Results

Establishment of a rat HUA model

Serum UA levels were measured by performing a clinical biochemical analysis. A three-fold increase in the serum UA concentration, from 1.89 μmol/L in control rats to 5.54 μmol/L in HUA rats, was observed, which indicated that we successfully created a rat HUA model (Fig. 1A).

HUA-induced MCI

With the increase in trial days, the escape latency of the two groups was shortened. In contrast to the normal control group, the escape latency of the HUA group was relatively longer (Fig. 1B), and the target quadrant residence time was shorter (Fig. 1C). Thus, HUA induces MCI in rats. The histopathological examination showed

inflammation in the hippocampus of the HUA group. The histological results indicated that the increasing inflammatory cells infiltrated into the hippocampus (Fig. 1G-I), inflammatory cells were observed in the hippocampus of HUA rats comparted to control group (Fig. 1D-F). Based on these histological results, the HUAD resulted in inflammation in the rat hippocampus.

Summary of Whole-transcriptome sequencing results

After the HUA model was established, we sent hippocampal samples from the control group and HUA group for whole-transcriptome sequencing to obtain a deeper understanding of HUA (Fig. 2). Whole genome sequencing produced 500.32 M raw reads (73.29 G bases) of data. After quality control and filtering, 496.04 M clean reads (70.61 G bases) were maintained for the subsequent analysis, with an average of 82.67 M reads and 11.77 G bases in each sample; the average GC level of the integrated sample was 46.93%. The general amount of rRNA was 26.56 M reads, which comprised an average of 3.52% of clean reads. The average GC content of the entire sample was 49.02%. The upper data indicate that we obtained high-quality RNA-seq statistics. Consequently, 93.04% of clean reads were mapped to the human reference genome, and the alignment rates at exonic, intronic, and intergenic regions were 53.90%, 28.13% and 18.08%, respectively. The Pearson correlation analysis and PCA chart was shown (Fig. 3A and B). Easily indicated that the correlation coefficient of approximately 88.89% of the sample was greater than 0.8, indicating a gene expression correlation for each sample.

Identification of differentially expressed ncRNAs

The gene fragments per kilobase million (FPKM) in each sample were calculated to conduct an analysis of differentially expressed genes [|log 2 (fold change) | value > 1, false discovery rate (FDR) < 0.05 was regarded as the threshold]. We identified 423 differentially expressed transcripts, which included 115 upregulated ncRNAs [log2 (fold change) > 1, FDR < 0.05] and 308 downregulated ncRNAs [log2 (fold change) < -1 FDR < 0.05] (Fig. 4A). These transcripts showed obviously disparate expression in the hippocampus between the HUA samples and control samples. Heatmaps of differentially expressed transcript clusters showed that these transcripts were significantly differentially expressed in the HUA and control samples (Fig. 4B). Compared with the control group, 391 mRNAs, 33 miRNAs, 31 lncRNAs and 8 circRNAs were differentially expressed in the HUA group. One hundred ten mRNAs, 7 miRNAs, 5 lncRNAs and 5 circRNAs were upregulated, while 281 mRNAs, 26 miRNAs, 26 lncRNAs and 3 circRNAs were downregulated in the HUA group.

Screening and analysis of differentially expressed mRNAs

Based on the established thresholds [log2 (fold change) > 0.585, FDR < 0.05], 391 differentially expressed mRNAs were screened, including 110 upregulated genes [log2 (fold change) > 0.585, FDR < 0.05] and 281 downregulated genes [log2 (fold change) <-0.585 FDR < 0.05] (Fig. 5A). All the differentially expressed genes showed significant changes in the HUA and control samples (Fig. 5B). These results indicate that the differentially expressed mRNAs we screened have obviously different characteristics. We executed an enrichment analysis and functional annotation of genes encoding differentially expressed mRNAs. The GO enrichment analysis annotated differentially expressed genes that were enriched in 388 biological processes (BPs), 62 cellular components (CCs), and 117 molecular functions (MFs) in the HUA group compared with the control group. Here, we chose the significant GO terms (*P* value < 0.01) in the BP-level GO results to construct the functional regulatory network (Fig. 5C). Afterwards, we chose the significant GO terms (*P* < 0.01) in the BP-level GO results to construct the functional regulation network (Fig. 6A). An in-depth analysis of enriched KEGG pathways indicated that the

differentially expressed genes (parental genes) in the HUA group were obviously associated with 23 KEGG pathways, including ECM-receptor interaction, PI3K-Akt signaling pathway, protein digestion and absorption, neuroactive ligand-receptor interaction and morphine addiction, compared with the control group. The top 20 KEGG pass ways are illustrated (Fig. 5D). The signal transduction relationship between pathways at the macro level was observed. We also discovered the core pathways affected by the experiment and regulatory mechanisms between signaling pathways (Fig. 6B).

Screening and analysis of differentially expressed lncRNAs, circRNAs and miRNAs

Similarly, in our study, 31 differentially expressed lncRNAs were identified, including 5 upregulated lncRNAs [log2 (fold change) > 1, FDR < 0.05] and 26 downregulated lncRNAs [log2 (fold change) < -1, FDR < 0.05]. Heatmaps of differentially expressed lncRNA clusters showed noticeable differences in the expression of these lncRNAs in the HUA and control samples (Fig. 7A-B). Eight differentially expressed circRNAs were obtained, of which 5 were upregulated and 3 were downregulated. Figure 7 shows the statistical (Fig. 7C) and cluster analyses (Fig. 7D) of the differentially expressed circRNAs. The differential expression analysis identified 33 differentially expressed miRNAs, including 7 upregulated and 26 downregulated miRNAs. Figure 7 also includes a volcano plot (Fig. 7E) and cluster analysis (Fig. 7F) of the differentially expressed miRNAs.

lncRNA ceRNA and circRNA ceRNA network maps

We used the 3 differentially expressed miRNAs with the most interactions (including 3 downregulated mRNAs, rno-miR-653-3p, rno-miR-351-5p, and rno-miR-322-5p) to recognize ceRNAs with the greatest plausible role in HUA. The network comprises 16 differentially expressed genes (downregulated genes included rno-miR-653-3p, rno-miR-351-5p, and rno-miR-322-5p; upregulated genes included Car12, Camkv, Tmem198, Pipn1, Dyrk2, Fibcd1, Crym, Ptpru, Syt17, Chst8, LOC100910821, LOC102548116, and LOC100911522). Two of the miRNAs were regulated by 1 differentially expressed lncRNA (Fig. 6C).

Verification of representative lncRNAs, miRNAs and mRNAs

Four mRNAs, one lncRNA and three miRNAs that emerged in the ceRNA network were chosen and verified using real-time quantitative polymerase chain reaction (RT-qPCR) to confirm the RNA-seq results. Crym, Fibcd1, Camkv, and Ptpru were upregulated. The results for the miRNAs showed that the expression of miR-653-3p, miR-322-5p and miR-351-5p was downregulated in the hippocampal samples from rats in the HUA group compared to the control rats. Meanwhile, the expression of LOC102548116 was upregulated in hippocampal samples from rats in the HUA group compared to control rats. Thus, the RT-qPCR results revealed that the relative expression levels of the selected ncRNAs were the same as the RNA-seq data (Fig. 8), indicating the reliability of the RNA-seq results.

Discussion

With the development of whole transcriptome analysis and molecular biotechnology, ncRNAs and mRNAs have attracted additional attention in the past few years [34]. Multiple studies have shown that ncRNAs play an essential role in different biological processes and are differentially expressed in many illnesses.

Our results are like previous reports that a higher level of SUA is cross-sectionally related to worse focus, operating memory, executive functioning, and psychomotor speed [7, 35, 36]. The current study first analyzed the whole transcriptome profiles of the hippocampus from HUA and normal rats using high-throughput sequencing and performed a subsequent evaluation of ncRNAs and mRNAs to identify the differentially expressed ncRNAs and mRNAs, as well as to investigate the latent biological features and the correlation between these ncRNAs, mRNAs and HUA.

A total of 25,834 RNAs was identified, comprising 15,701 mRNAs, 680 miRNAs, 3,354 lncRNAs and 6,108 circRNAs. Most remarkably, 1 KEGG pathway was related to injury to the brain, and various types of N-glycan biosynthesis signaling pathways were related to asparagine (including high-mannose type glycans, N-glycans, paucimannose type glycans and glycohormones). Among these pathways, glycohormones play an essential role in the production of asparagine. An analysis of the major KEGG results revealed that the pathways related to the formation of asparagine were among the most substantially altered. A previous study also proposed that asparagine endopeptidase (AEP) is a lysosomal cysteine proteinase that is activated during aging and proteolytically reduces tau, abolishes its microtubule fitting characteristics, and triggers neurodegeneration and tau aggregation [37].

Although significant findings were reported in these studies, restrictions should also be noted. In our research, we analyzed data from 6 groups of rats, and since one of the samples was obviously different from the other groups, we excluded this sample from subsequent analyses. In summary, we identified a particular degree of HUA injury to the hippocampus at the genetic level. Changes in gene expression led to changes in gene equilibrium and the expression of molecules involved in various signaling pathways. These results improve our understanding of the global genetic responses to HUA in the rat hippocampus and provide a novel theoretical basis and tactics to treat HUA-induced MCI using gene therapy.

We analyzed 3 differentially expressed miRNAs (rno-miR-653-3p, rno-miR-351-5p and rno-miR-322-5p). Their correlations were regulated by several lncRNAs and circRNAs, such as Chst8 (up)-, rno-miR-322-5p (down)-, and LOC100911522-derived lncRNAs (up). This finding suggests that the mechanism of HUA is regulated by many ceRNAs.

Conclusions

We concluded that HUA is associated with particular models of gene expression and the activation or suppression of hippocampal signaling pathways. A definite level of HUA can induce injury to the hippocampus at the genetic level. These consequences thus provide a new theoretical foundation and strategy to treat arthrolithiasis or other diseases associated with HUA using gene therapy.

Materials And Methods

All methods were carried out in accordance with relevant guidelines and regulations.

Ethics statement

The studies were conducted in compliance with ARRIVE guidelines 2.0 (https://arriveguidelines.org/). and in compliance with all applicable guidelines and regulations. During the experiment, all animal-related procedures

were performed following related guidelines and regulations of the Ethics Committee for Animal Research of the Southwest Minzu University (Approval No.2019-12). Animals were handled in rigorous accordance with good animal practice, and all effects were made to relieve unnecessary suffering and distress of animals. All animal experiments were conducted according to the regulations for the Administration of Affairs Concerning Experimental Animals (Ministry of Science and Technology, China, revised in June 2004).

Construction of the rat HUA model

Specific pathogen-free (SPF) male Wistar rats (7–8 weeks old; 180–220 g weight) were purchased from Vital River Laboratories. Twenty-four rats were separated and housed in groups of 2 per cage in clear plastic cages with wire grid lids in a colony with a 12 h light and dark cycle (lights on from 7:00 A.M. to 7:00 P.M.) in an invariable environment with a temperature of (22 ± 2) ℃, humidity (55 ± 5) %, and noise < 85%. The animals were provided free access to food and water. We provided the HUAD containing 2% UA and 2% oxonic acid (OA) to rats for periods ranging from 1 day to 12 weeks to establish the HUA model, while the rats in the control group were provided normal basic feed. In this study, we performed a statistical analysis 6 groups of rats, and because the sample size was small and one of the samples was obviously different from the other, we excluded this group in the subsequent analyses; thus, we may have underestimated the changes.

Serum biochemical analysis

After anesthetizing with intraperitoneal injection of pentobarbital sodium (20 g/140 μL), rats were euthanatized then blood and hippocampal tissues were harvested for subsequent experiments. Serum was obtained after coagulation (4°C, 60 min) and centrifugation (3000 r/min, 15 min, 4°C). A clinical chemical analysis of the serum was carried out using a Cobas C 311 biochemistry analyzer (Basel, Switzerland) purchased by F. Hoffmann-La Roche, Ltd., and appropriate kits with the following parameters: SUA. Serum biochemical test reagents were purchased from Mike Industrial Co., Ltd. (Chengdu, Sichuan, China). All assays of biochemical parameters were performed in strict accordance with the instructions provided with the corresponding blood biochemical kit.

Determination of learning and memory function in rats

All rats were allowed to practice finding the fixed platform for 5 successive days (4 trials/day). Afterwards, rats were allowed to circumnavigate the pool and search for the hidden platform for a maximum of 60 sec. The latencies were recorded, and the progress of the test was video-taped. On day 5, the rats were offered a 60 sec test to determine whether they retained the spatial location of the platform. We recorded the numbers of animals crossing the exact location of the platform and the time spent in the target quadrant.

Histological examination

Hippocampal specimens were fixed with neutral-buffered 4% paraformaldehyde, embedded in paraffin wax, and sectioned. We stained the sections of paraffin-embedded hippocampal tissues with hematoxylin-eosin for the histological analysis, and observed the results using an Olympus BX53F microscope (Olympus, Japan) equipped with a DP80 digital camera.

High-throughput sequencing

Six hippocampal samples (three from the HUA group and three from the control group) were designated for the whole transcriptome analysis using high-throughput sequencing. All analyses of RNA-Seq data were conducted

with the assistance of NovelBio Bio-Pharm Technology Co., Ltd. (Shanghai, China). The summary data of RNA-seq are listed in Table 1.

Table 1
Summary of RNA-seq data

Sample	Raw reads	Clean reads	Ratio (%)	GC (%)	Mapped ratio (%)	Exonic (%)	Intronic (%)	Intergenic (%)
Control1	91242138	90807840	99.52	46.78	93.7	55.65	26.59	17.90
Control2	92601642	92143398	99.50	46.86	93.2	50.78	31.20	18.15
Control3	104445682	103940076	99.51	46.83	92.5	47.30	33.96	18.85
Hyperuricemia1	87488902	87066068	99.51	46.93	93.4	58.69	23.51	17.93
Hyperuricemia2	73345770	71971916	98.13	46.42	92.6	53.98	28.46	17.69
Hyperuricemia3	75498478	74206686	98.29	47.74	92.7	59.21	23.21	17.72
Total	500.32M	496.04M	/	/	/	/	/	/
Average	83.39M	82.67M	99.08	46.93	93.02	54.27	27.82	18.04

Quality control

First, we used Fast-QC (http://www.bioinformatics.babraham.ac.uk/projects/fastqc/) software for an overall evaluation of the quality of the sequencing data, including the quality of base value distribution, quality value position distribution, GC content, RT-qPCR duplicate content, and KMER frequency. These evaluation metrics allowed us to obtain insights into the sequencing data itself prior to the mutation detection.

Mapping statistics

We use Hisat2 software to compare RNA-seq data with database version Rnor6. Hisat2 is an efficient and fast RNA-seq data analysis tool, a new index building method based on BWT and small-scale indexing that is built every 56 kb, combined with adjustment strategies that quickly and accurately locate each read to a site in the genome. These small indexes are combined with some adjustment strategies that quickly and accurately locate each read ratio in the genome. Hisat2 support genomes of any size. For miRNA mapping, we used an internationally recognized BWA algorithm to compare the filtered CleanRead to the sheep miRbase (http://www.mirbase.org/) [38, 39] database and to the Rfam database. Furthermore, we predicted the potential miRNAs.

The GO analysis and pathway analysis

GO analysis is mainly used to query gene functions and relationships between functions and genes that perform the functions based on GO (http:\\www.geneontology.org\). The mRNAs examined in the differential mRNA and ceRNA analyses were annotated based on the database, and all the GO terms in which the genes were enriched were obtained using Fisher's test to compute the significance level (*P* value) of each GO. The differentially expressed mRNAs and mRNAs were identified in the ceRNA analysis using the database to access all the genes involved in GO terms. Fisher's exact test was used to calculate the *P* value of each GO and to screen the

significant GO terms with different enriched genes with the condition of $P < 0.05$. Generally, Fisher's exact test is utilized to categorize GO terms by calculating the FDR to calibrate the P value.

A pathway analysis is an approach to detect significant pathways in which differentially expressed genes are involved according to gene annotation databases, and thus we performed a pathway analysis to query the signal transduction pathways and regulatory relationships in which genes were involved using KEGG (http://www.genome.jp/Kegg/) to download pathway annotations of microarray-identified genes. Accordingly, the critical goal of the pathway analysis is to obtain a complete database and complete pathway annotations. Initially, pathway annotation was performed on the differentially expressed mRNAs and mRNAs identified in the ceRNA analysis based on the KEGG database to assess all the pathways in which the genes were involved. Fisher's exact test based on a hypergeometric distribution was used to calculate the P value of each pathway, and then the significant pathways represented by different genes were screened with $P < 0.05$ as the standard.

Coexpression network

Currently, gene coexpression networks are widely used to investigate the system-level functions of genes [40]. We integrated the predicted target genes to ensure the lncRNA/circRNA, miRNA and mRNA results from the joint analysis of the same lncRNAs/circRNAs and the same level of up- and downregulation. The ceRNA joint networks were constructed using Cytoscape [41]. The ceRNA network discloses the patterns and features of different ncRNAs, as well as the regulatory relationships between various ncRNAs that bind to common miRNA binding sites to regulate gene expression through miRNA sponge mechanisms [42]. Then, we constructed gene co expression networks based on the normalized signal intensity of specifically expressed genes. We calculated the Pearson correlation coefficients and selected the significantly correlated pairs to construct the network for each pair of genes.

RNA extraction and quantitative PCR

In this validation step, we selected 10 hippocampal samples from the HUA group (n = 5) and control group (n = 5) to verify 8 significantly differentially expressed ncRNAs using RT-qPCR. Total RNA was extracted from rat hippocampal samples using TRIzol reagent (Takara, Dalian, China) according to the manufacturer's protocol. RNA was transcribed into cDNAs using Prime Script™ II Reverse Transcriptase (Takara) according to the manufacturer's instructions. RT-qPCR was performed using SYBR1 Premix Ex Taq™ II (Takara) according to the manufacturer's protocol with a Step One Plus™ Real-Time PCR System (ABI, Applied Biosystems, Foster City, CA). Gene expression was calculated using the 2-ΔΔCt method [43]. All experiments were performed independently three times. The RT-qPCR primer sequences are listed in Table S1.

Statistical analysis

Data reported in this study are presented as the means ± standard deviations. Student's t-test was used to verify the differences between two groups. The association between samples was analyzed using Pearson's correlation analysis. GraphPad 9.0 was employed to draw graphs. P value < 0.05 was considered statistically significant.

Abbreviations

MCI: Mild cognitive impairment; RNA-Seq: RNA-sequencing; DEGs: Differentially expressed genes; ceRNA: Competitive endogenous RNA; qRT-PCR: Quantitative real-time polymerase chain reaction; UA: Uric acid; HUA: Hyperuricemia; SUA: Serum uric acid; MWM: Morris water maze; ncRNA: Noncoding RNA; CRP: C-reactive protein;

TLR4: Toll-like receptor 4; mRNA: Message RNAs; miRNA: Micro RNA; lncRNA: Long non-coding RNA; circRNA: Circular RNA; HUAD: High-UA diet; FPKM: Fragments per kilobase million; FDR: False discovery rate; BPs: Biological processes; CCs: Cellular components; MFs: Molecular functions; GO: Gene Ontology; KEGG: Kyoto Encyclopedia of Genes; SPF: Specific pathogen-free; OA: Oxonic acid; AEP: Asparagine endopeptidase;

Declarations

Authors' contributions

XNS conceived and designed the study and coordination, revised it critically for important content. PKH and NL performed the statistical analysis, prepared the figures and tables and drafted the manuscript. MA carried out the conserved domains and gene analysis and helped to prepare the figures and tables. BHZ, XYM and QLJ analyzed the data. HCX collected specimens. XNS participated in the design of this study and statistical analysis. All authors read and approved the final manuscript.

Funding

This work was supported by National Natural Science Foundation of China (No. 81801086); Fundamental Research Funds for the Central Universities, Southwest Minzu University (No. 2019HQZZ19).

Availability of data and materials

The datasets used and/or analysed during the current study are available from the corresponding author on reasonable request.

Declarations

Ethics approval and consent to participate

The studies were conducted in compliance with ARRIVE guidelines 2.0 (https://arriveguidelines.org/). and in compliance with all applicable guidelines and regulations. During the experiment, all animal-related procedures were performed following related guidelines and regulations of the Ethics Committee for Animal Research of the Southwest Minzu University (Approval No.2019-12). Animals were handled in rigorous accordance with good animal practice, and all effects were made to relieve unnecessary suffering and distress of animals. All animal experiments were conducted according to the regulations for the Administration of Affairs Concerning Experimental Animals (Ministry of Science and Technology, China, revised in June 2004).

Competing interests

The authors have declared that no competing interests exist.

References

1. Wang J, Qin T, Chen J, Li Y, Wang L, Huang H, Li J. Hyperuricemia and risk of incident hypertension: a systematic review and meta-analysis of observational studies. PloS one. 2014; 9(12): e114259.
2. Fathallah-Shaykh SA, Cramer MT. Uric acid and the kidney. Pediatr Nephrol (Berlin, Germany). 2014;29(6):999-1008.

3. Ashihara H, Stasolla C, Fujimura T, Crozier A. Purine salvage in plants. Phytochemistry. 2018; 147:89-124.
4. Villegas R, Xiang YB, Elasy T, Xu WH, Cai H, Cai Q, Linton MF, Fazio S, Zheng W, Shu XO. Purine-rich foods, protein intake, and the prevalence of hyperuricemia: the Shanghai Men's Health Study. Nutrition, metabolism, and cardiovascular diseases: NMCD. 2012; 22(5):409-416.
5. Kaneko K, Aoyagi Y, Fukuuchi T, Inazawa K, Yamaoka N. Total purine and purine base content of common foodstuffs for facilitating nutritional therapy for gout and hyperuricemia. Biol Pharm Bull. 2014; 37(5):709-721.
6. Choi HK, Liu S, Curhan G. Intake of purine-rich foods, protein, and dairy products and relationship to serum levels of uric acid: the Third National Health and Nutrition Examination Survey. Arthritis Rheum. 2005; 52(1):283-289.
7. Vannorsdall TD, Kueider AM, Carlson MC, Schretlen DJ. Higher baseline serum uric acid is associated with poorer cognition but not rates of cognitive decline in women. Exp Gerontol. 2014; 60:136-139.
8. Zhu X, Raina AK, Perry G, Smith MA. Alzheimer's disease: the two-hit hypothesis. The Lancet Neurol. 2004; 3(4):219-226.
9. de Oliveira EP, Burini RC. High plasma uric acid concentration: causes and consequences. Diabetol Metab Syndr. 2012; 4:12.
10. Rock KL, Kataoka H, Lai JJ. Uric acid as a danger signal in gout and its comorbidities. Nat Rev Rheumatol. 2013; 9(1):13-23.
11. Lohsoonthorn V, Dhanamun B, Williams MA. Prevalence of hyperuricemia and its relationship with metabolic syndrome in Thai adults receiving annual health exams. Arch Med Res. 2006; 37(7):883-889.
12. Greenberg JD, Reed G, Kremer JM, Tindall E, Kavanaugh A, Zheng C, Bishai W, Hochberg MC. Association of methotrexate and tumour necrosis factor antagonists with risk of infectious outcomes including opportunistic infections in the CORRONA registry. Ann Rheum Dis. 2010; 69(2):380-386.
13. Nagahama K, Iseki K, Inoue T, Touma T, Ikemiya Y, Takishita S. Hyperuricemia and cardiovascular risk factor clustering in a screened cohort in Okinawa, Japan. Hypertens Res. 2004; 27(4):227-233.
14. Ames BN, Cathcart R, Schwiers E, Hochstein P. Uric acid provides an antioxidant defense in humans against oxidant- and radical-caused aging and cancer: a hypothesis. Proc Natl Acad Sci U. S. A. 1981; 78(11):6858-6862.
15. Sautin YY, Johnson RJ. Uric acid: the oxidant-antioxidant paradox. Nucleosides, nucleotides & nucleic acids 2008; 27(6):608-619.
16. Mikami T, Sorimachi M. Uric acid contributes greatly to hepatic antioxidant capacity besides protein. Physiol Res. 2017; 66(6):1001-1007.
17. El Ridi R, Tallima H. Physiological functions and pathogenic potential of uric acid: A review. J Adv Res. 2017; 8(5):487-493.
18. Nigam SK, Bhatnagar V. The systems biology of uric acid transporters: the role of remote sensing and signaling. Curr Opin Nephrol Hypertens. 2018; 27(4):305-313.
19. Kuo CF, Grainge MJ, Mallen C, Zhang W, Doherty M. Rising burden of gout in the UK but continuing suboptimal management: a nationwide population study. Ann Rheum Dis. 2015; 74(4):661-667.
20. Zhu Y, Pandya BJ, Choi HK. Prevalence of gout and hyperuricemia in the US general population: the National Health and Nutrition Examination Survey 2007-2008. Arthritis Rheum. 2011; 63(10):3136-3141.

21. da Silva FC, Iop RDR, de Oliveira LC, Boll AM, de Alvarenga JGS, Gutierres Filho PJB, de Melo L, Xavier AJ, da Silva R. Effects of physical exercise programs on cognitive function in Parkinson's disease patients: A systematic review of randomized controlled trials of the last 10 years. PloS one. 2018; 13(2):e0193113.
22. Shao X, Lu W, Gao F, Li D, Hu J, Li Y, Zuo Z, Jie H, Zhao Y, Cen X. Uric Acid Induces Cognitive Dysfunction through Hippocampal Inflammation in Rodents and Humans. J Neurosci: the official journal of the Society for Neuroscience 2016; 36(43):10990-11005.
23. Vorhees CV, Williams MT. Morris water maze: procedures for assessing spatial and related forms of learning and memory. Nat Protoc. 2006; 1(2):848-858.
24. Squire LR. Memory and the hippocampus: a synthesis from findings with rats, monkeys, and humans. Psychol Rev 1992; 99(2):195-231.
25. Jiang Z, Zhou X, Li R, Michal JJ, Zhang S, Dodson MV, Zhang Z, Harland RM. Whole transcriptome analysis with sequencing: methods, challenges and potential solutions. Cell Mol Life Sci. CMLS 2015; 72(18):3425-3439.
26. Black S, Kushner I, Samols D. C-reactive Protein. J Biol Chem. 2004; 279(47):48487-48490.
27. Dogan S, Piskin O, Solmaz D, Akar S, Gulcu A, Yuksel F, Cakır V, Sari I, Akkoc N, Onen F. Markers of endothelial damage and repair in Takayasu arteritis: are they associated with disease activity? Rheumatol Int. 2014; 34(8):1129-1138.
28. Mukherjee S, Huda S, Sinha Babu SP. Toll-like receptor polymorphism in host immune response to infectious diseases: A review. Scand J Immunol. 2019; 90(1):e12771.
29. Okun E, Barak B, Saada-Madar R, Rothman SM, Griffioen KJ, Roberts N, Castro K, Mughal MR, Pita MA, Stranahan AM. Evidence for a developmental role for TLR4 in learning and memory. PloS one 2012; 7(10):e47522.
30. Kawai T, Akira S. Signaling to NF-kappaB by Toll-like receptors. Trends Mol Med. 2007; 13(11):460-469.
31. Daneman R, Prat A: The blood-brain barrier. Cold Spring Harbor Perspect Biol. 2015; 7(1): a020412.
32. Feig DI, Kang DH, Johnson RJ. Uric acid and cardiovascular risk. N Engl J Med. 2008; 359(17):1811-1821.
33. Jin M, Yang F, Yang I, Yin Y, Luo JJ, Wang H, Yang XF. Uric acid, hyperuricemia and vascular diseases. Front Biosci-Landmark. 2012; 17:656-669.
34. Forrest AR, Carninci P. Whole genome transcriptome analysis. RNA Bio. 2009, 6(2):107-112.
35. Vannorsdall TD, Jinnah HA, Gordon B, Kraut M, Schretlen DJ. Cerebral ischemia mediates the effect of serum uric acid on cognitive function. Stroke. 2008; 39(12):3418-3420.
36. Schretlen DJ, Inscore AB, Jinnah HA, Rao V, Gordon B, Pearlson GD. Serum uric acid and cognitive function in community-dwelling older adults. Neuropsychol. 2007; 21(1):136-140.
37. Panosyan EH, Wang Y, Xia P, Lee WN, Pak Y, Laks DR, Lin HJ, Moore TB, Cloughesy TF, Kornblum HI et al. Asparagine depletion potentiates the cytotoxic effect of chemotherapy against brain tumors. Mol Cancer Res. MCR 2014; 12(5):694-702.
38. Griffiths-Jones S. miRBase: the microRNA sequence database. Methods Mol Biol (Clifton, NJ). 2006; 342:129-138.
39. Griffiths-Jones S, Saini HK, van Dongen S, Enright AJ. miRBase: tools for microRNA genomics. Nucleic Acids Res. 2008; 36(Database issue): D154-158.

40. Zhang B, Horvath S. A general framework for weighted gene co-expression network analysis. Stat Appl Genet Mol Biol. 2005; 4: Article17.
41. Shannon P, Markiel A, Ozier O, Baliga NS, Wang JT, Ramage D, Amin N, Schwikowski B, Ideker T. Cytoscape: a software environment for integrated models of biomolecular interaction networks. Genome Res. 2003; 13(11):2498-2504.
42. Tang L, Li P, Li L. Whole transcriptome expression profiles in placenta samples from women with gestational diabetes mellitus. J Diabetes Invest. 2020; 11(5):1307-1317.
43. Livak KJ, Schmittgen TD. Analysis of relative gene expression data using real-time quantitative PCR and the 2(-Delta Delta C(T)) Method. Methods. 2001; 25(4):402-408.

Figures

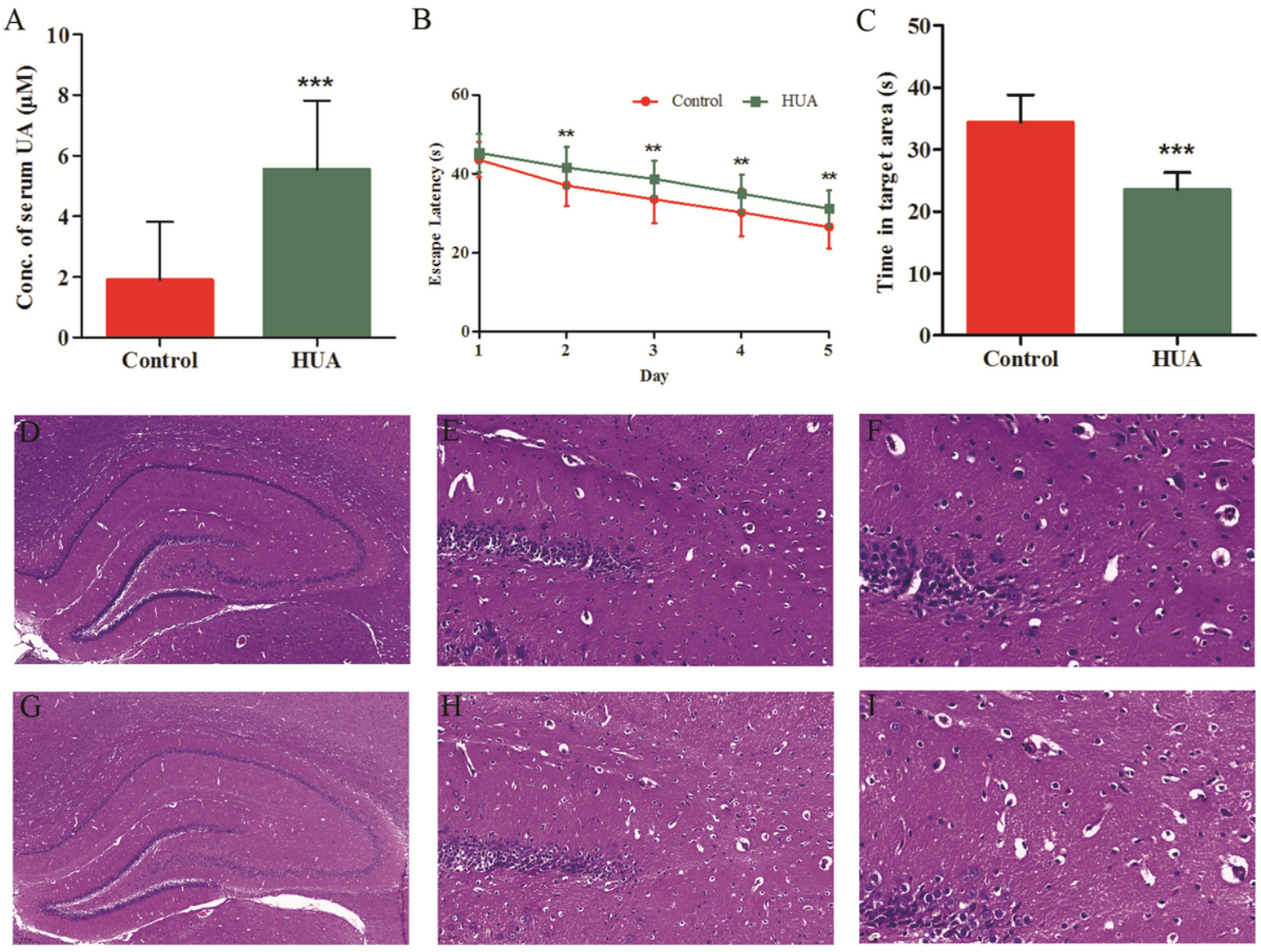

Figure 1

Characteristics of rats fed a normal or HUA diet and the results of the Morris water maze test. **A.** Differences in the SUA concentration and **B.** Escape latency. **C.** Time spent in the target area of the Morris water maze test were observed. $^{**}P < 0.01$ and $^{***}P < 0.001$ compared with the control group. The hippocampus of HUA rats showed

clear inflammation. **D.** Microscopic images of the hippocampus of the control group × 5 magnification. **E.** Control group × 10 magnification. **F.** Control group × 20 magnification. **G.** HUA group × 5 magnification. **H.** HUA group × 10 magnification. **I.** HUA group × 20 magnification.

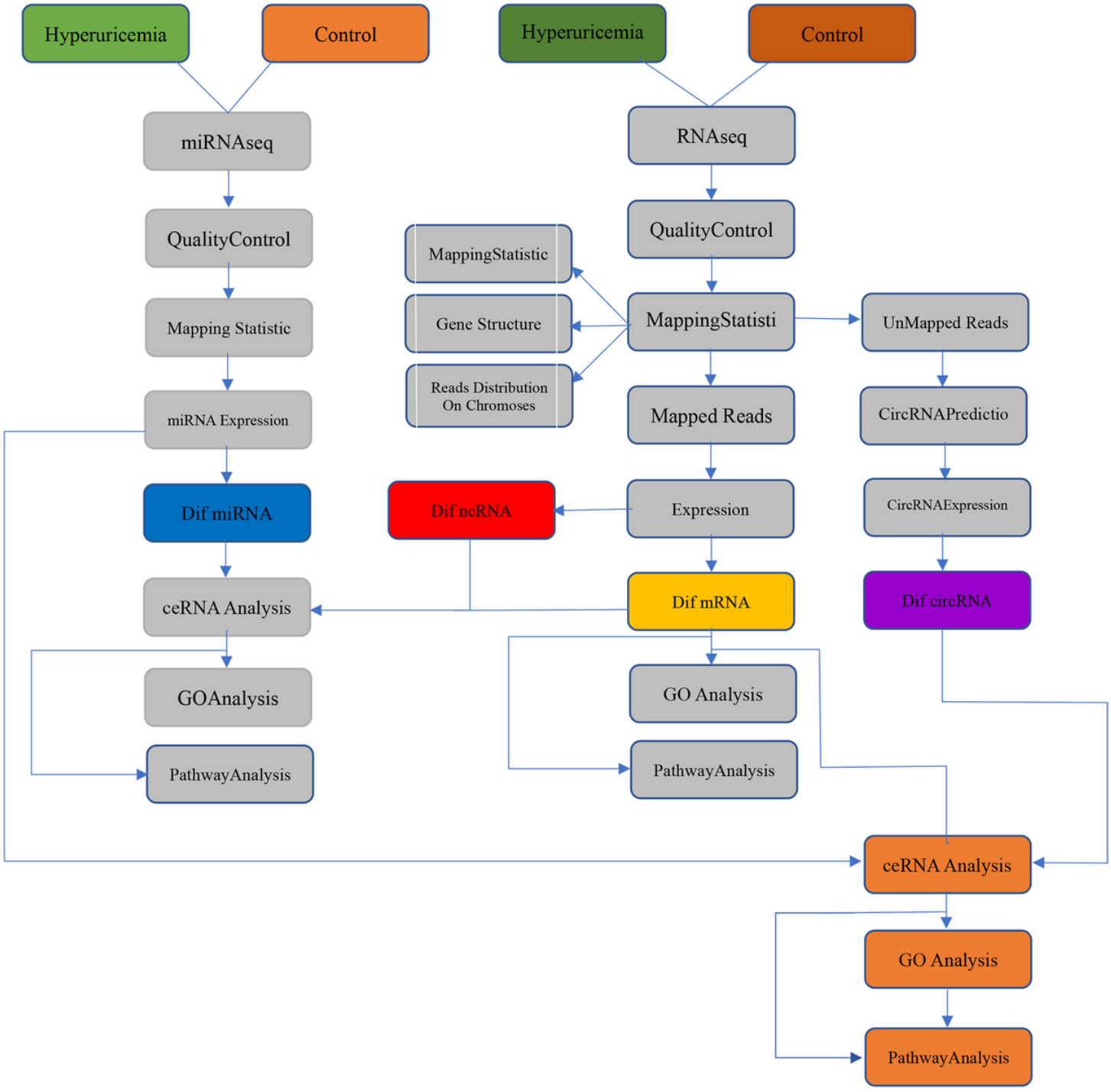

Figure 2

Flowchart for the whole transcriptome sequencing analysis.

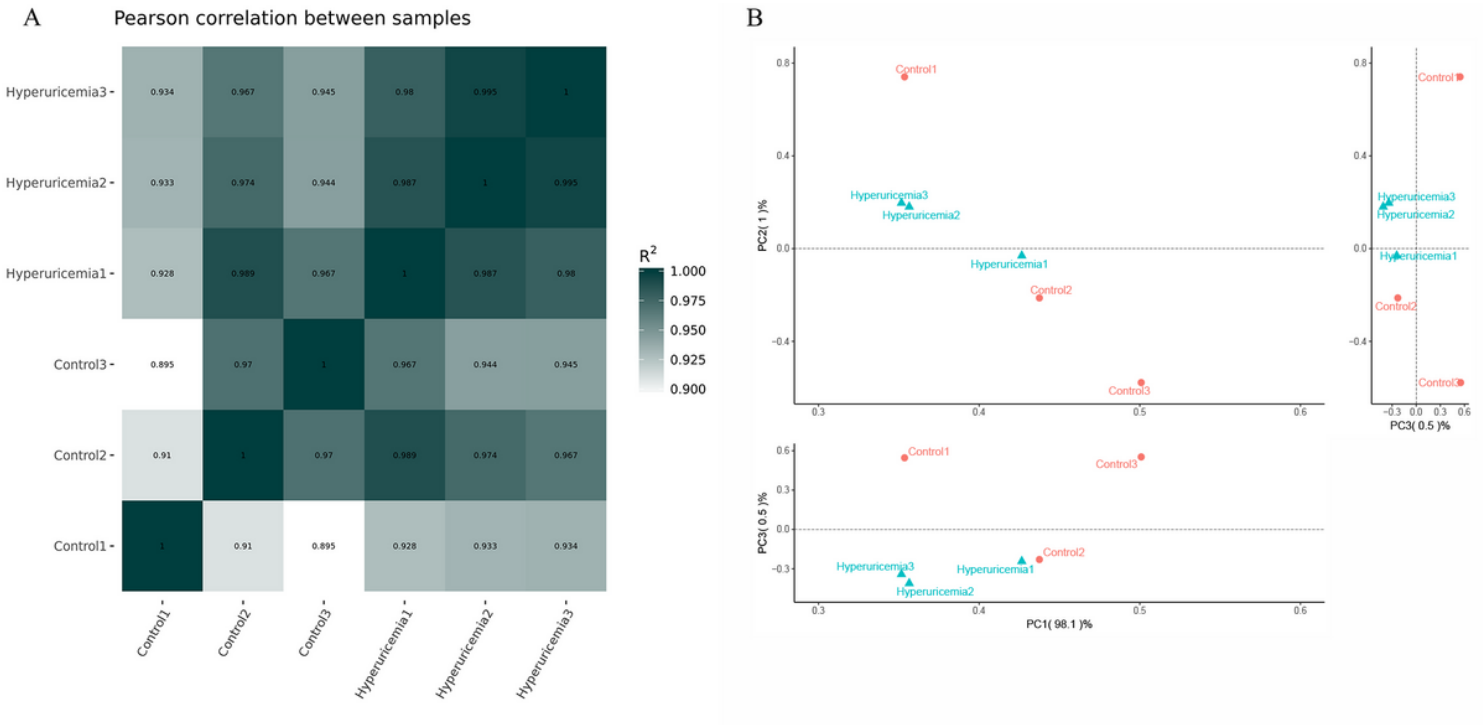

Figure 3

The Pearson correlation coefficients between samples and principal component analysis. **A.** Pearson's correlation coefficients (PCCs) between samples; the closer the R^2 value is to 1, the stronger the correlation between samples. **B.** Principal component analysis (PCA).

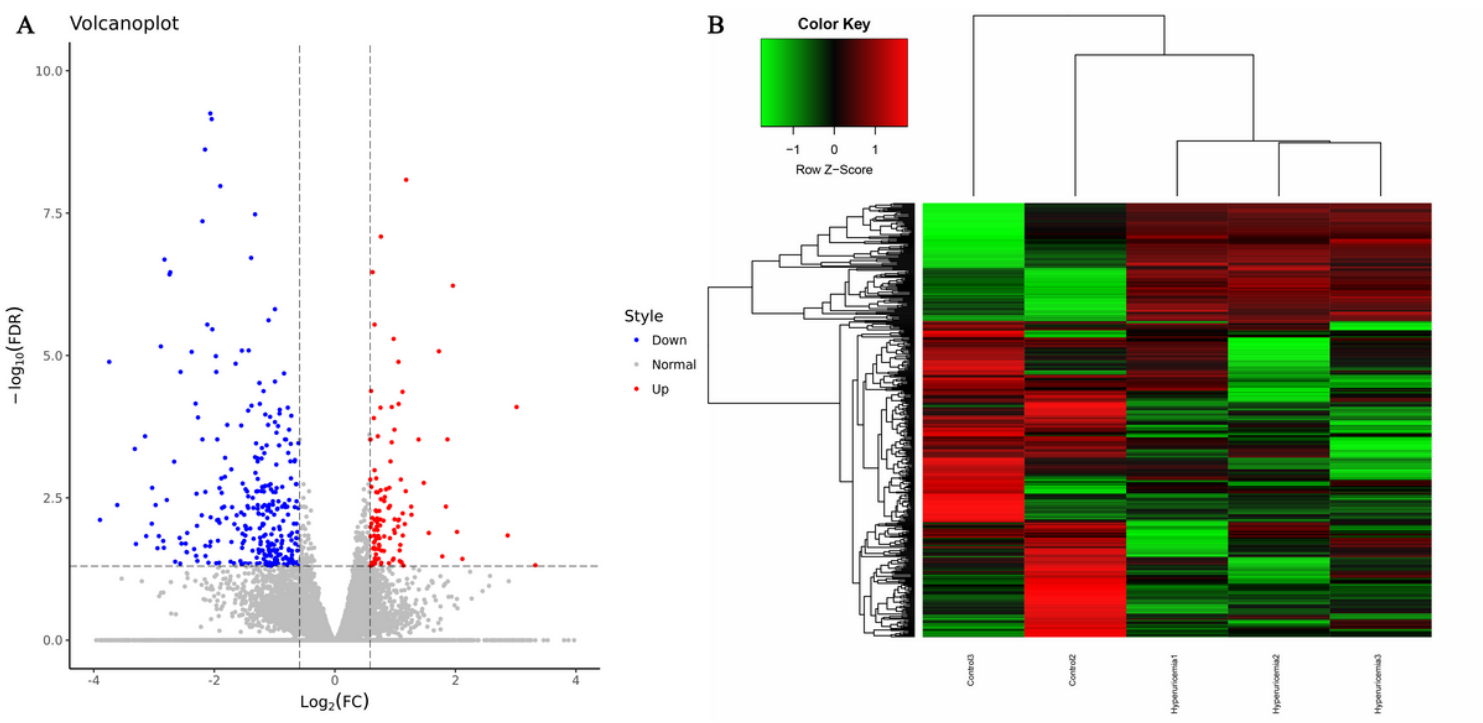

Figure 4

Identification and further analysis of DEGs in the hippocampus of MCI rats compared with control rats. **A.** Volcano plot comparing HUA rats and the rats in the control group. Red points indicate upregulated RNAs [log2 (fold change) > 1, FDR < 0.05], while blue nodes indicate downregulated ncRNAs [log2 (fold change) > -1, FDR < 0.05]. Gray dots refer to normally expressed ncRNAs. **B.** A heatmap analysis was performed to determine differential expression between the HUA group and the control group. Each line represents a single ncRNA, and each column represents a tissue sample.

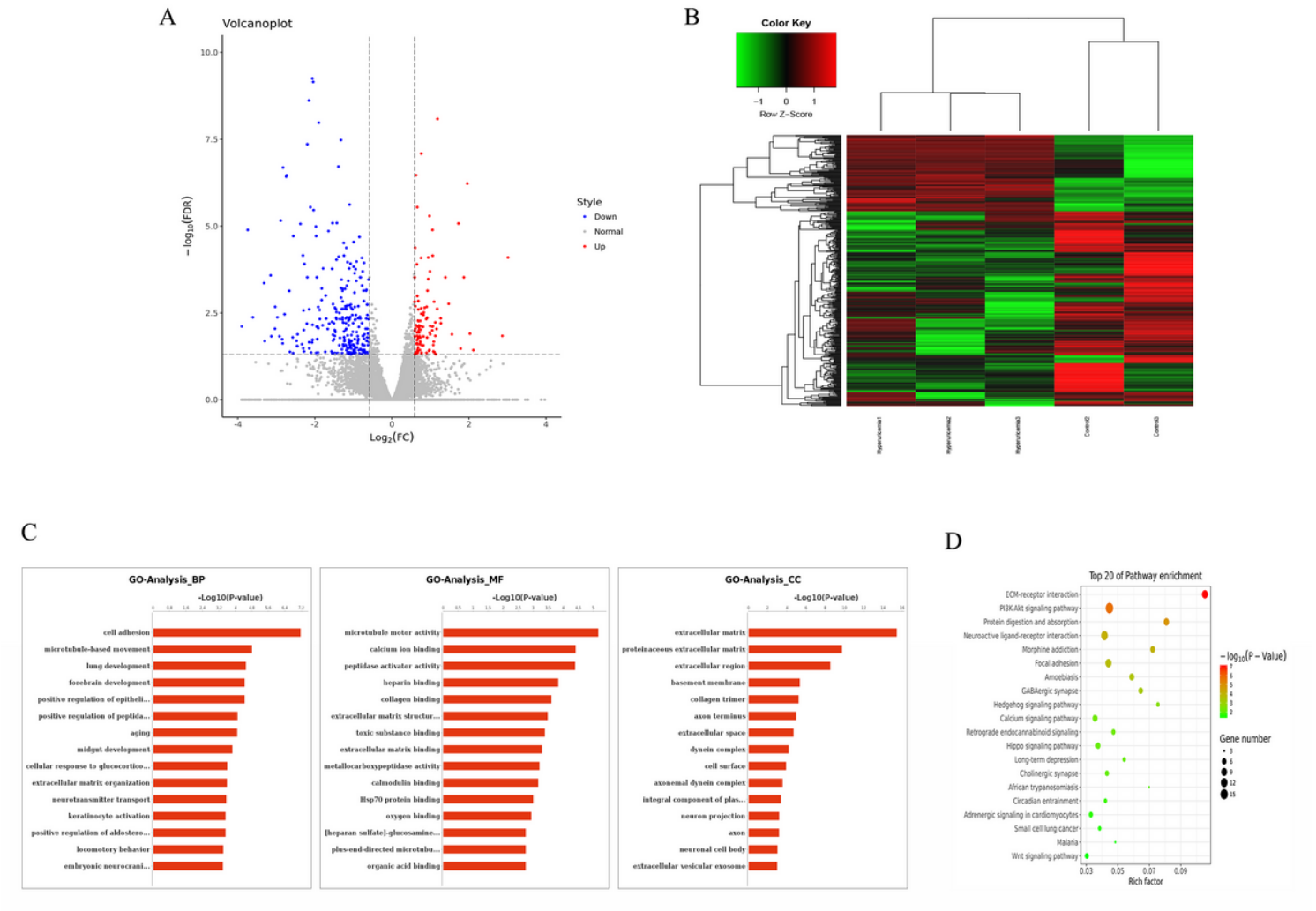

Figure 5

The identification and further analysis of DEGs in the hippocampus of MCI rats compared with control rats. **A.** Volcano plot comparing HUA rats and the rats in the control group. Red points indicate upregulated mRNAs [log2 (fold change) > 1, FDR < 0.05], while blue nodes indicate downregulated mRNAs [log2 (fold change) > -1, FDR < 0.05]. Gray dots refer to normally expressed mRNAs. **B.** A heatmap analysis was performed to determine the differentially expressed genes between the HUA group and the control group. Each line indicates a single mRNA, and each column indicates a tissue sample. **C.** Gene Ontology analysis of DEGs, including MF, CC and BP classifications. The horizontal axis represents the enrichment value at the functional level, and the vertical axis represents the entry name corresponding to the GO term in the Gene Ontology database. **D.** Kyoto Encyclopedia of Genes and Genomes pathway analysis of DEGs. The size of the bubble shows the number of genes related to the pathways; the bubble color indicates the *P* value.

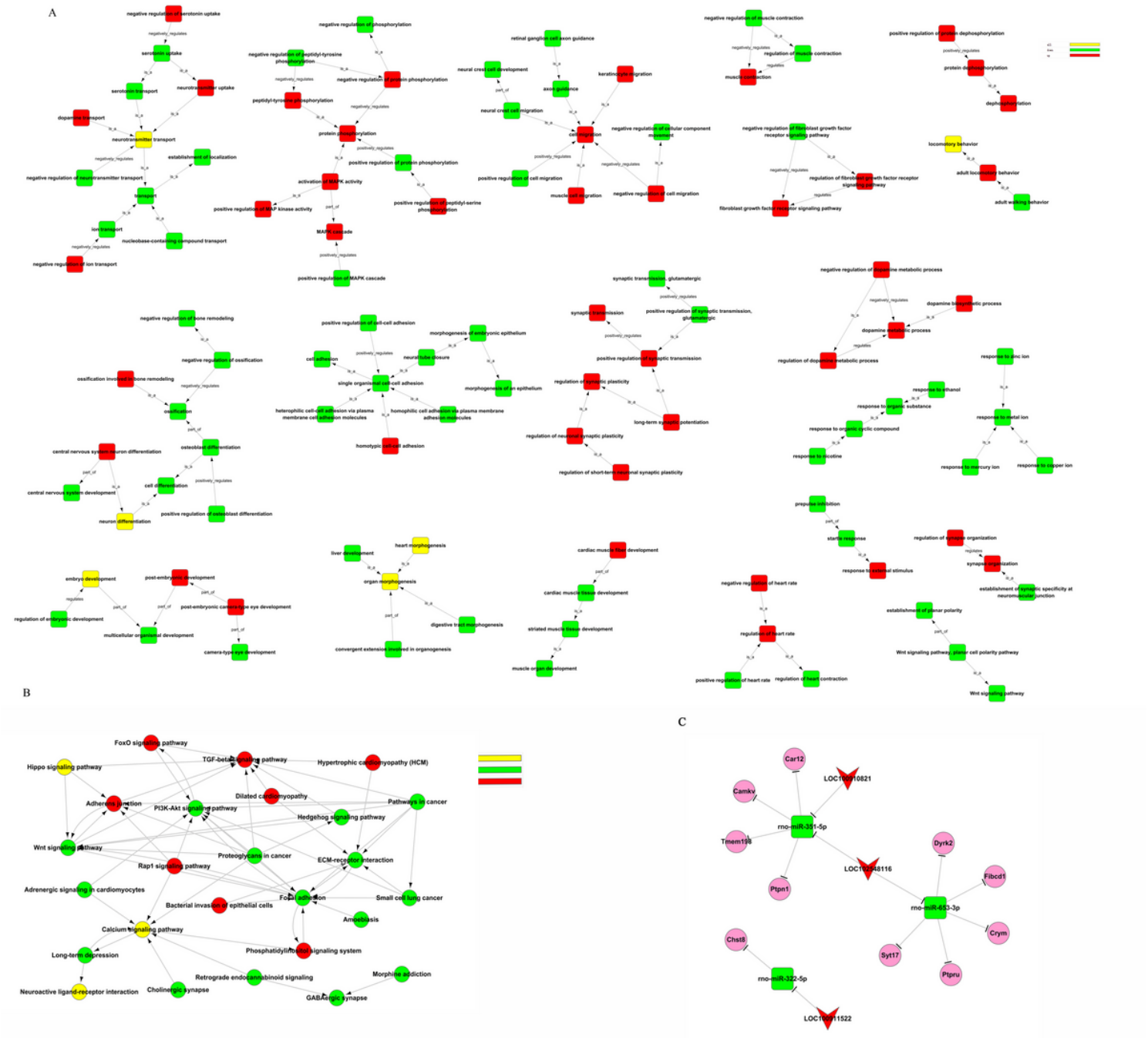

Figure 6

Hierarchical tree diagram of salient functions and signaling pathway regulatory networks and the competing endogenous RNA network for the 3 miRNAs with maximum interactions. **A.** Hierarchical tree diagram among salient functions and GO trees of significant GO terms ($P < 0.01$). Green indicates significant GO terms in which downregulated genes are enriched, red indicates significant GO terms in which upregulated genes are enriched, and yellow indicates significant GO terms in which both upregulated and downregulated genes are enriched. **B.** Signaling pathway regulatory network. The up- and downregulated pathway terms are shown ($P < 0.05$). Green indicates the significant pathway term enriched in downregulated genes, red indicates the significant pathway term enriched in upregulated genes, and yellow indicates the significant pathway term enriched in both upregulated and downregulated genes. **C.** The lncRNA-miRNA-mRNA competing endogenous RNA network. Multiple colors represent up- and downregulation of miRNAs, lncRNAs and mRNAs in the HUA sample compared

with the control group. Vee, rounded rectangle, and ellipse represent differentially expressed lncRNAs, miRNAs and mRNAs, respectively.

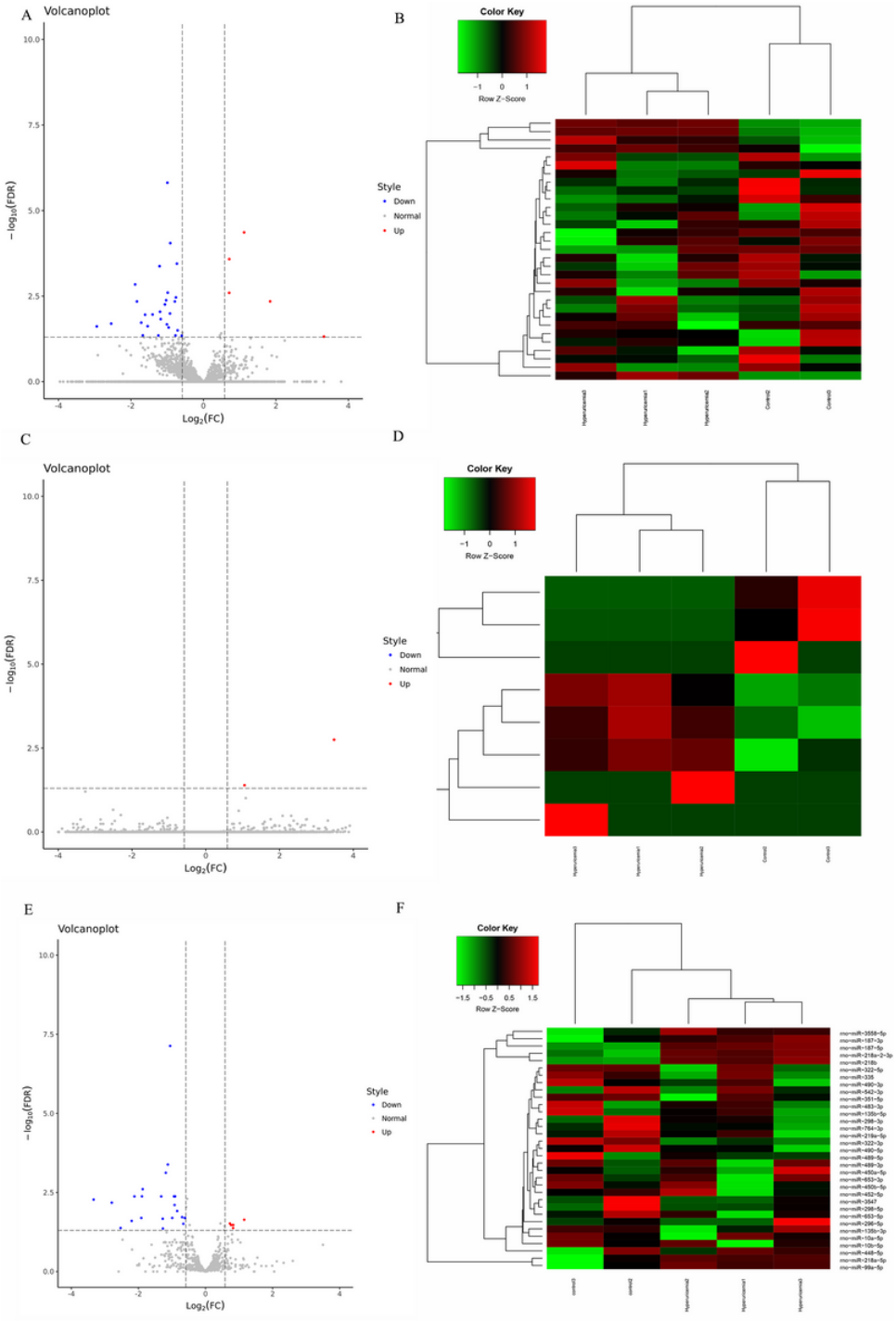

Figure 7

Differentially expressed lncRNAs, miRNAs and circRNAs in the rat renal HUA model. Volcano plot of differentially expressed lncRNAs (**A**), miRNAs (**C**) and circRNAs (**E**) between rats suffering from HUA and normal control rats. Red nodes refer to lncRNAs that were upregulated [log2 (fold change) > 1, FDR < 0.05], while blue nodes represent lncRNAs that were downregulated [log2 (fold change) < -1, FDR < 0.05]. Gray points indicate the lncRNAs and miRNAs showing normal expression. Hierarchical clustering analysis of lncRNAs (**B**), miRNAs (**D**) and circRNAs

(**F**). showing differential expression between the HUA group and the control group. The closer the color to red, the higher of expression. In contrast, green denotes downregulated expression profiles.

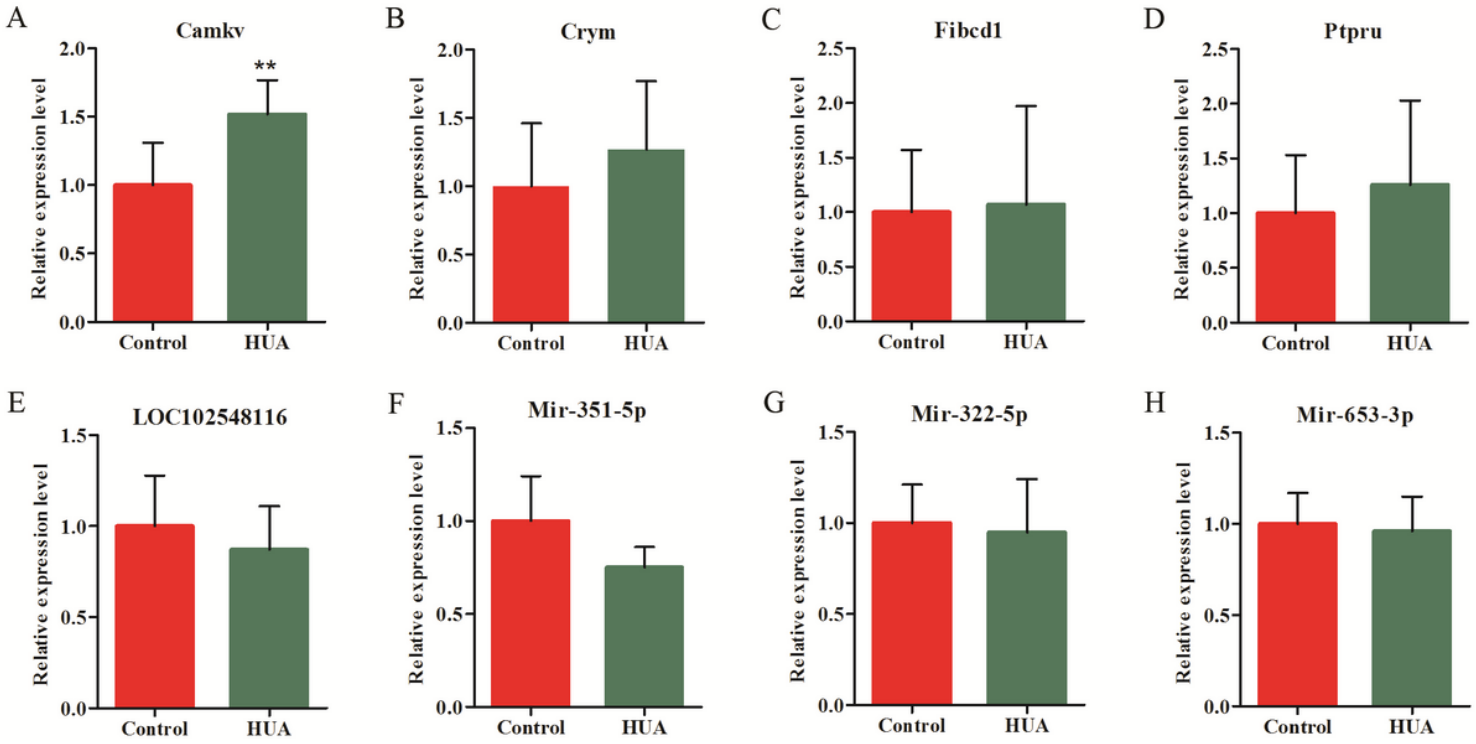

Figure 8

RT-qPCR validation of representative mRNAs, lncRNAs and miRNAs. The relative expression of mRNAs (**A-D**), lncRNAs (**E**) and miRNAs (**F-H**) were validated in hippocampal samples from HUA rats (n = 5) and control rats using RT-qPCR for comparison to the RNA-seq results. Student's t-test was used to compare quantitative data between groups. Variance in means was considered statistically significant at $*P < 0.05$.

Supplementary Files

This is a list of supplementary files associated with this preprint. Click to download.

- SupplementaryTable.docx